Supporting Information for: Universal Radiative Lifetimes in the Long-Lived Luminescence of Si Quantum Dots

Tomáš Popelář,[†] Pavel Galář,[†] Filip Matějka,[†] Giacomo Morselli,[‡] Paola Ceroni,[‡] and Kateřina Kůsová[†*,]

[†]*Institute of Physics of the ASCR, v.v.i., Cukrovarnická 10, 162 00 Prague 6, Czechia*
[‡] *Chemistry Department "Giacomo Ciamician", Via F. Selmi 2, University of Bologna, 40126 Bologna, Italy*

E-mail: kusova@fzu.cz

S1 Compilation of literature data

A set of literature data by Miura et al.,[1] Greben et al.[2] and Valenta et al.[3] were combined with our measurements to deduce the ideal fully radiative average lifetimes $\tau_{\mathrm{PL}}^{\mathrm{ideal}}$ from Figure 1(d). Two studies which also report fully radiative average lifetime by Sangghaleh et al[4] and Kalkman et al[5] were not included in the calculation because their reported values are slightly lower than the remaining datasets, see Figure 2b. Radiative lifetimes reported by Liu et al.[6] are a simplistic recalculation from QY measurements, disregarding the influence of dark QDs. Therefore, they were not included either.

All the lifetimes included in the figure were recalculated into average lifetimes τ_{PL} using Eq. (5). The stretched-exponential parameters were extracted from the text where available, or the reported PL decays were digitalized and re-fitted.

In the study by Miura et al,[1] the reported radiative rates are based the τ_{SE} stretched-exponential lifetime and thus they also needed to be recalculated. A typical β for high-quality samples of 0.85 was assumed, which corresponds to the $\Gamma(2/\beta)/\Gamma(1/\beta) \approx 1.3$ factor connecting the stretched-exponential and average lifetimes. Thus, the plots used to deduce the radiative and non-radiative rates by Miura et al.[1] were digitalized, corrected by this factor and re-fitted to yield the average rates rather than the stretched-exponential rates. Based on the comparison between these values, the correction factor of 1.36 was applied to the radiative lifetimes reported by Miura et al.[1]

Data by Greben et el[2] and Valenta et al[3] report intensity-averaged rates, so no recalculation to the average lifetimes was necessary. However, these decays were acquired using significantly different experimental conditions (long-pulse excitation), which are known to lead to longer lifetimes when compared to classical fast excitation.[7] Thus, data obtained from these studies[2,3] were corrected by a factor of 0.85. The corresponding correction factor for short-pulse excitation can be determined by comparison of the decay times after sufficiently short and sufficiently long excitation,[7] with the "long" decay time being ≈ 283 µs and the "short" decay time ≈ 250 µs. Out of the datasets presented in the latter study,[3] only the deduced radiative rates were included here.

To ensure equal weight of the individual measurements in the characterization of the universal lifetime curve $\tau_{\mathrm{PL}}^{\mathrm{ideal}}(\lambda)$, all the datasets were first interpolated so that each one contained roughly 25 evenly spaced points within the measured interval of emission photon ener-

gies. In order to characterize the value of the $^1/_{k_{QC}}$ slope parameter as accurately as possible, each dataset was first fitted with an exponential and the mean value and the standard deviation of these k_{QC} values was calculated. In a second run, this mean k_{QC}^{exp} value was fixed and a second exponential fit for all the data assuming the $^1/_{k_{QC}^{exp}}$ slope was used to extract the A_{PL}^{exp} offset parameter (reported with 66 % confidence bands).

S2 Intensity-averaged photoluminescence lifetimes

Using strictly its definition, the intensity averaged lifetime[8]

$$\tau_{PL}(\lambda) = \frac{\int_0^\infty tI(t,\lambda)\,\mathrm{d}t}{\int_0^\infty I(t,\lambda)\,\mathrm{d}t} \tag{S1}$$

is an emission-photon-energy dependent number characterizing the lifetime of an PL decay independently of the fitting model. In a single-exponential PL decay $I(t) = I_0 \exp(-^t/_{\tau_{exp}})$, τ_{PL} from Eq. (S1) equals directly the $^1/_e$ decay time ($\tau_{PL} = \tau_{exp}$) and for many common shapes of the PL decay curve, average τ_{PL} can be easily calculated using a simple analytical formula.[8] More generally, for a multi-exponential fit composed of N exponentials $I(t) = \sum_{i=0}^{N} I_i \exp(-^t/_{\tau_i})$, the average lifetime τ_{PL}^{ME} is equal to[2]

$$\tau_{PL}^{ME} = \frac{\sum_{i=0}^{N} I_i \tau_i^2}{\sum_{i=0}^{N} I_i \tau}. \tag{S2}$$

In a stretched-exponential PL decay, τ_{PL} combines τ_{SE} and β for a given emission photon energy λ into a single parameter[8]

$$\tau_{PL} = \frac{\Gamma(^2/_\beta)}{\Gamma(^1/_\beta)}\tau_{SE}, \tag{S3}$$

where $\Gamma()$ is the gamma function. Thus, it is possible to calculate the model-independent average lifetime $\tau_{PL}(\lambda)$ from Eq. (S1) very simply by traditional fitting of a set of PL decays at different emission photon energies using a stretched-exponential function from Eq. (4) and then inserting the τ_{SE} and β parameters directly into Eq. (5). Notably, the fit of the same curve assuming a different mathematical models leads to very similar values of lifetimes.[2]

S3 Details about PL decay measurements

The trends reported on in this study are based on a large number of measurements with varying experimental conditions (excitation intensity $10^{24} - 10^{26}$ $^{ph}/_{cm^2 s}$, mode of excitation: fs or ns laser and excitation wavelength: 315 – 400 nm, two-photon or two-step excitation at 515 and 780 nm) with no significant deviations from the reported average lifetimes except for the influence of measurement and analysis artifacts, such as the lowering of the determined average lifetimes due to low PL signal.[9] On the whole, at least 90 PL maps, corresponding to at least 2,000 individual PL decays, were experimentally characterized and their behavior analyzed. This relatively large statistical sample ensures the robustness of the observed universality of PL decays and is crucial for our ability to identify measurement- or analysis-induced artifacts in the determination of the average lifetimes.

Possible artifacts in the determination of $\tau_{PL}(\lambda)$ in Figure 1c are connected with (i) the inaccurate determination of the PL onset time, (ii) the omission of the longer-timescale tail of the PL decay, (iii) underestimation of the influence of the solvent for example via stray light in the detector and (iv) excessive noise in the data. Whereas issue (i) can generally skew the results of a fit in any direction,[9] the latter three issues lead to the underestimation of the extracted lifetimes.[9] Therefore, we included the onset of PL in our analysis and made sure that the tail of the PL decay was accurately measured. To properly visualize the PL tail, the PL decays are plotted in an offset logarithmic vertical scale, where a small constant is added to the PL signal before applying the logarithmic scale to ensure that the signal is non-negative

and its whole range shows in the logarithmic plot (inset of Figure 1a).[9]

S4 The determination of non-radiative lifetimes

To illustrate the role of the A_{PL} parameter, we can imagine a set of SiQDs in which the lifetimes of the non-radiative processes are comparable to those of the radiative ones $\tau_r = \tau_{nr}$. In such a set of samples, the corresponding measured τ_{PL} will be about a half of that of the ideal $\tau_{\mathrm{PL}}^{\mathrm{ideal}}(\lambda)$ curve from Figure 1(c), because $\tau_{\mathrm{PL}} = {}^{1}\!/_{({}^{1}\!/_{\tau_r}+{}^{1}\!/_{\tau_r})} = {}^{\tau_r}\!/_{2}$. This difference will be reflected in the A_{PL} parameter as $A_{\mathrm{PL}}(\tau_{nr} = \tau_r) = {}^{A_{\mathrm{PL}}(\tau_{nr}\to\infty)}\!/_{2} = {}^{A_{\mathrm{PL}}^{\mathrm{exp}}}\!/_{2}$.

The A_{PL} value allows us to roughly estimate, disregarding the underlying λ dependence, the magnitude of microsecond non-radiative lifetimes in the "non-ideal" etch-SiQD:Oa sample. As $A_{\mathrm{PL}}^{\mathrm{etch-SiQD:Oa}} \approx {}^{A_{\mathrm{PL}}^{\mathrm{exp}}}\!/_{5}$ and the ${}^{1}\!/_{k_{\mathrm{QC}}}$ slope is very close to ${}^{1}\!/_{k_{\mathrm{QC}}^{\mathrm{exp}}}$, the etch-SiQD:Oa non-radiative lifetimes are roughly ${}^{1}\!/_{4}$ of those of the purely radiative $\tau_{\mathrm{PL}}^{\mathrm{ideal}}$ curve (${}^{1}\!/_{\tau_{\mathrm{PL}}^{\mathrm{etch-SiQD:Oa}}} = {}^{5}\!/_{\tau_{\mathrm{PL}}^{\mathrm{ideal}}} = {}^{1}\!/_{\tau_r}{}^{\mathrm{ideal}} + {}^{4}\!/_{\tau_r}{}^{\mathrm{ideal}} \Rightarrow \tau_{nr}^{\mathrm{etch-SiQD:Oa}} = {}^{\tau_{\mathrm{PL}}^{\mathrm{ideal}}}\!/_{4}$). The corresponding iQY is 0.2.

S5 The accuracy of the determination of the stretched-exponential stretching parameter

In order to assess the influence of the data quality, namely the signal-to-noise ratio and data sparsity, on the fitted parameters, we define two quantities as follows. These quantities are determined from the underlying measured data $I(t, \lambda)$ and the parameters of fitted function $f(t, \lambda)$, in particular of the onset times $t_0(\lambda)$ and the average measured lifetimes $\tau_{\mathrm{PL}}(\lambda)$. To ensure that the two quantities are independent of the overall temporal length of the measurement window, they are determined on a temporal interval of a sufficiently high signal T^{signal}, which we define as the interval between the onset time t_0 and three times of the average lifetime τ_{PL} from data onset

$$T^{\mathrm{signal}} \in \langle t_0, t_0 + 3\tau_{\mathrm{PL}} \rangle. \tag{S4}$$

A time interval defined in this way sufficiently covers the decay of the signal for both the exponential and the stretched-exponential curves.

Firstly, the N/S parameter describing the noise-to-signal ratio of a decay curve $I(t)$ is determined from the standard deviation (std{}) of the residuals of the fit on the T^{signal} interval after being normalized for the maximum (max{}) of the fitted decay curve $f(t)$

$$N/S = \left. \frac{\mathrm{std}\left\{I(t) - f(t)\right\}}{\max\left\{f(t)\right\}} \right|_{t \in T^{\mathrm{signal}}}. \tag{S5}$$

A visual representation this definition is given in Figure S1(a). Using the maximum of the fitting function in the denominator of this formula rather than normalizing simply for the maximum of data ensures that the N/S parameter is not influenced by potential noise spikes around the maximum of the measured data. Secondly, the sparsity of data N^{signal} is characterized simply as the number of datapoints inside the T^{signal} internal. Please note that each decay $I(t)$ is characterized by a single N/S and a single N^{signal} parameter, which makes both these parameters potentially dependent on the emission wavelength λ. Examples of decay curves with the corresponding data quality parameters are shown in Figure S1(b).

Further, we used synthetically generated decay curves such as the ones in Figure S1 to assess how the data-quality parameters defined above influence the output of data analysis. To generate the synthetic curves $f_{\mathrm{synth}}(t)$, a function with known parameters $f_{\mathrm{real}}(\beta_{\mathrm{real}}, \tau_{\mathrm{real}}; t)$ was calculated for a selected number of equally sampled datapoints and randomly generated noise following the normal distribution was added

$$f_{\mathrm{synth}} = f_{\mathrm{real}} + \mathrm{noise}. \tag{S6}$$

In an ideal case, fitting of the f_{synth} curve would recover the ($\beta_{\mathrm{real}}, \tau_{\mathrm{real}}$ parameters of the f_{real} function. However, if the random noise and sparser data have non-negligible influence on the fitting procedure, the parameters obtained

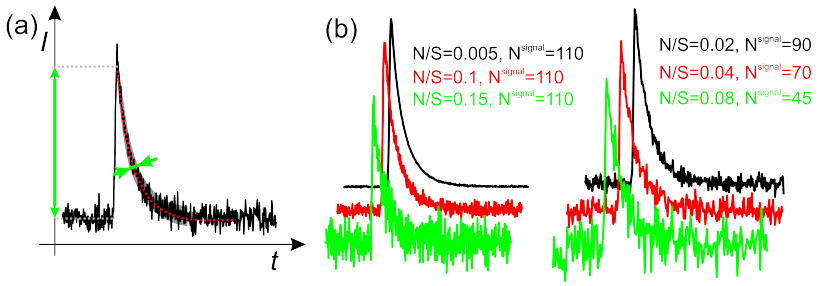

Figure S1: (a) Visual representation of Eq. (S5) (b) Examples of decay curves characterized by various N/S and N^{signal}.

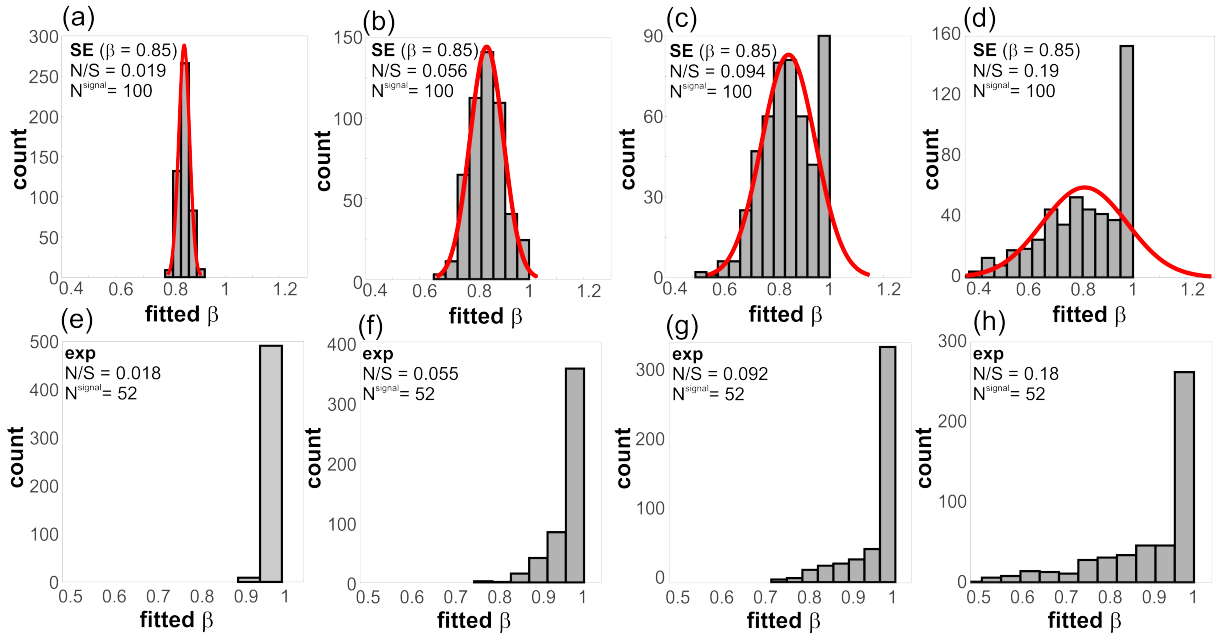

Figure S2: Examples of histograms of β's fitted to synthetic decay curves with known parameters and added noise (each histogram represents the statistics of 500 decay curves). (a–d) The underlying data follow a stretched-exponential decay with $\beta = 0.85$, $N^{\text{signal}} = 100$ and N/S varies. The histogram is overlaid with a fit to a normal distribution in red. (e–h) The underlying data follow a single-exponential decay, $N^{\text{signal}} = 52$, N/S varies.

by fitting the synthetic curve would be different from the ($\beta_{\mathrm{real}}, \tau_{\mathrm{real}}$ "real" ones. These synthetic datasets then underwent a standard[9] fitting procedure assuming a stretched-exponential decay, which allowed us to extract the statistics of fitted β_{fit} parameters and statistically determine how a particular random pattern of noise influences the extracted decay curves. In the following analysis, only the influence of the data quality on the β_{real} parameter is discussed, because the β dispersion parameter determines the "nature" of PL decay (single-exponential, non-single-exponential).

One possibility of describing the statistics of the fitted β_{fit}'s is simply using histograms as in Figure S2. Histograms of fitted β_{fit}'s for an underlying stretched-exponential decay ($\beta_{\mathrm{real}} = 0.85$) presented in Figure S2(a–d) clearly illustrate how, intuitively, the histogram gets broadened for noisier datasets. The distribution of β_{fit}'s would closely resemble a normal distribution but, when performing a stretched-exponential fit, the upper bound for β_{fit} is traditionally set to one. This upper bound artificially crops the histogram as it gets broader (Figure S2(c,d)). Figure S2 clearly illustrates how a non-negligible percentage of fits naturally converge to $\beta_{\mathrm{fit}} = 1$ or other, "incorrect" ($\beta_{\mathrm{real}} \neq 0.85$) values of β, even if the underlying dataset f_{real} follows a stretched-exponential decay as a result of lower-quality data (sparser datapoints, higher level of noise).

In the reverse case, when the underlying synthetic data $f_{\mathrm{real}}(t)$ are single-exponential and are fitted with a stretched-exponential function as in Figure S2(e–h), the fit often converges to $\beta_{\mathrm{fit}} = 1$, in other words to a single-exponential. However, as the data gets noisier, a tail of fitted $\beta_{\mathrm{fit}} < 1$ again broadens (Figure S2(g,h)). This noise-induced deviation of the fit from the shape of the underlying dataset can be quantified by calculating the portion of β_{fit}'s which falls outside of the interval $\beta_{\mathrm{fit}} \in \langle \beta_{\mathrm{real}} - 0.05, \beta_{\mathrm{real}} + 0.05 \rangle$ (or the interval $\langle 0.9, 1 \rangle$ for a single exponential), which will be referred to as p. The p parameter can be interpreted as the rough estimate of the probability that the fitted β_{fit} parameter differs from the real underlying decay β_{real} by more than 0.05 as a result of data sparsity and the presence of noise. Thus, $p \to 0$ implies high certainty about the β_{fit} value, while $p \to 0.3$ signifies about a 30% probability of the fitted β_{fit} being incorrect. Using our analysis as presented above, we constructed a dependence of the p parameter of the data quality parameters N/S and N^{signal}. We found out that p relatively strongly depends on the noise-to-signal ratio N/S, see Figure S3(a), but its dependence on data sparsity N^{signal} is weaker. Based on the shape of this dependence, solely for the purposes of a simple description, we selected a fitting function well-describing p for N/S and N^{signal} parameter values relevant for PL decay measurements as follows

$$p(A, w; N/S, N^{\mathrm{signal}}) = A\left[1 - \frac{w^2 N^{\mathrm{signal}}}{(N/S)^2 + w^2 N^{\mathrm{signal}}}\right], \tag{S7}$$

where A and w are parameters which are derived from the above analysis and depend on the parameters of the underlying, real data. Whereas A represents the value to which p "asymptotically" approaches for noisier data ($N/S \to 0.3$ and more), the weakly N^{signal}-dependent w denotes the N/S value where p attains half of this maximum. A simplified two-dimensional example disregarding the $p(N^{\mathrm{signal}})$ dependence of the $p(N/S)$ dependence in Figure S3(a). The whole $p(N/S, N^{\mathrm{signal}})$ dependence for an underlying single-exponential ($\beta_{\mathrm{real}} = 1$) and stretched-exponential ($\beta_{\mathrm{real}} = 0.85$) PL decays is then shown in Figure S3(b), the corresponding parameters are listed in Table S1. Whereas in the single-exponential decay curve, the probability p of the fitted β_{fit} to be outside of the $\langle 0.9, 1 \rangle$ interval slowly rises to roughly 35 % with increasing N/S noise value as the tail of the histogram in Figure S2(e–h) broadens, a possible error in β_{fit} for a stretched-exponential decay rises to an even higher value with the analogical histogram broadening. Changing β_{real} from 0.85 to 0.75 influences the fit deviation p only marginally, see Table S1.

In our analysis, we use a mode of fitting including the onset of the PL decay, as we discussed elsewhere.[9] However, in most PL decays

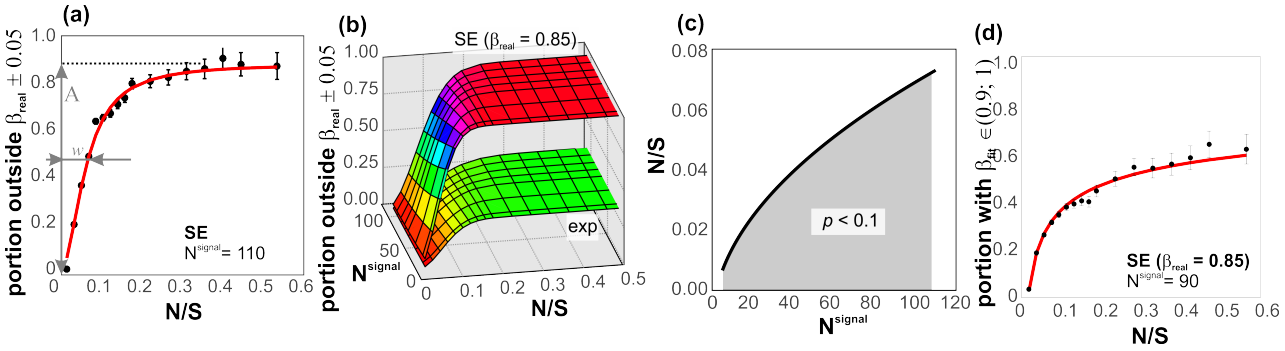

Figure S3: (a) The dependence of p, the portion of β_{fit} falling outside of the $\langle \beta_{\text{real}} - 0.05; \beta_{\text{real}} + 0.05 \rangle$ interval, on the noise-to-signal ratio N/S on an example of a stretched-exponential synthetic decay ($\beta_{\text{real}} = 0.85$,$N^{\text{signal}}$ =110). The red curve represents the fit by a formula $A\left(1 - \frac{w^2}{(N/S)^2+x^2}\right)$, whose generalized version including both N/S and N^{signal} is shown as Eq. (S8). (b) The summary of the deviations of the fitted β_{fit} for a single-exponential (exp) and a stretched-exponential underlying PL decay from Figure S2 using $p(N/S, N^{\text{signal}})$ from Eq. (S8) (the corresponding parameters are listed in Table S1). One $p(N/S, N^{\text{signal}})$ dependence was calculated using a statistics of 68,000 synthetic PL decay curves. (c) The gray area highlights noise levels and number of datapoints in the dataset for a fitted β_{fit} value to be statistically significant ($p < 0.1$ in Eq. (S8)). (d) The portion of β_{fit} converging to $\langle 0.9; 1 \rangle$ for underlying stretched-exponential data ($\beta_{\text{real}} = 0.85$, $N^{\text{signal}} = 90$), the data are fitted using Eq. (S9).

Table S1: The parameters of Eq. (S8) for various combinations of underlying PL decay data and fitting approaches.

underlying data	β_{real}	fit	A	w
exponential	1.0	SE	0.37	1.4×10^{-2}
SE	0.85	SE	0.90	6.3×10^{-3}
SE	0.75	SE	0.90	9.3×10^{-3}

reported in the literature, this PL onset is excluded from the data, which results in the uncertainty about the onset time where the PL decay starts and thus produces much larger errors of the fitted parameters.[9] We performed the fit quality assessment in the same way as presented above also for fitting excluding PL onset. The analysis revealed that the mode of fitting impacts the $p(N/S, N^{\text{signal}})$ dependence. In particular, if care is taken to use an "appropriate" onset time when fitting without the PL onset, the p values for noisier data $N/S > 0.5$ approach somewhat lower values than those presented in Figure S3(b) (i.e. As from Table S1 are lower) and the initial rise is much steeper in the case of an exponential underlying dataset (w is lower). However, the histograms of β_{fit} for noisier and sparser data are much less ordered than for the case of onset-included fitting in Figure S2 as the fit deviations are no longer solely statistical errors of a single parameter (β_{fit}). Thus, we will use the $p(N/S, N^{\text{signal}})$ dependence derived using the onset-included fitting for a rough fit-quality assessment in general. Since the onset-included mode of fitting is much more reliable, the corresponding noise-induced error can only be underestimated in this way, never overestimated.

The presented analysis provides us with a tool to determine if a possible noise-induced error of a stretched-exponential β_{fit} obtained from a non-linear least-square fitting is small enough to provide reasonable certainty about the fitted value. If we consider a $p = 0.1$ probability that the β_{fit} is outside ± 0.05 range (other values can be chosen), we can calculate the acceptable noise-to-signal level for a particular datasets from Eq. (S8)

$$\begin{aligned} (N/S) &< \frac{w}{\sqrt{A-p}}\sqrt{N^{\text{signal}}} \Rightarrow \\ N/S &\lessapprox 0.05 \text{ for } N^{\text{signal}} = 50, \\ N/S &\lessapprox 0.07 \text{ for } N^{\text{signal}} = 100. \end{aligned} \tag{S8}$$

These threshold noise levels are depicted in Figure S3(c). If the data-quality parameters N/S and N^{signal} are outside of the designated range, a stretched-exponential fit cannot reliably distinguish between an exponential and a stretched-exponential curve.

One more important quantity to be deduced from the described analysis is the percentage p_{exp} of fits in which the fit incorrectly converges to a single-exponential ($\beta_{\text{fit}} \in \langle 0.9; 1 \rangle$) for underlying stretched-exponential data ($\beta_{\text{real}} = 0.85$). This quantity can be easily estimated from the already-calculated set of β_{fit} histograms from Figure S2(a–d). This dependence takes on an analogical but slightly different shape than the one in Figure S3(a), as shown in Figure S3(d). To represent the slightly different shape we describe this dependence using a formula

$$p_{\text{exp}}(A, w; N/S) = 1 - \frac{A}{(N/S)^w} \tag{S9}$$

with $A = 0.35$ and $w = 0.25$. In this case, the dependence on N^{signal} is too weak to play a role.

The variability the histograms in Figure S1 indicates one possibility of circumventing this limitation: the histograms of β_{fit} are shaped differently for an underlying stretched-exponential and exponential data. (We note, however, that this difference significantly smears if onset-excluded fitting is applied.) Thus, constructing a histogram of β_{fit} will hint at the underlying PL decay. The disadvantage of this approach is the relatively large number of independent datasets necessary for such an analysis, making it difficult to be applied.

S6 Example of the comparison of individual PL lifetimes to the ideal curve

Measured PL lifetimes in the average notation τ_{PL} from Eq. (5) of any sample can be easily compared to the fully radiative $\tau_{\text{PL}}^{\text{ideal}}$ curve, see Figure S4.

One example of the need to discuss the uncertainty in the determined β parameter are the single-QD PL decays.[10] In SiQDs, in contrast to direct-bandgap materials, the measurements of single-QD PL decays are notori-

ously difficult due to the extremely low emission rates arising from microsecond PL decays ($\tau_{\mathrm{PL}} \approx {}^{1}/_{10^{-4}}\ \mathrm{s}^{-1} \rightarrow 10^{4}\ {}^{\mathrm{photons}}/_{\mathrm{s}}$), implying that the detection system needs to be extremely sensitive and optimized for the signal to overcome noise. Consequently, noise level are also important in the interpretation of the results and a closer inspection is necessary before concluding that the observed single PL decay was single-exponential.[10] In the PL decays presented in that paper, we could estimate the fit ambiguity coefficients p_{exp}. When assuming an exponential fit, p is relatively large ($p_{\mathrm{exp}} \approx 0.3$). However, both these datasets can be also well fitted using a stretched-exponential function ($\beta \approx 0.7$ and 0.8, respectively). The application of a stretched-exponential fit in turn significantly increases the resulting fit ambiguity coefficient ($p_{\mathrm{SE}} \approx 0.6$ and 0.8, respectively). Thus, our analysis supports the proposed conclusion that the reported PL decays are single-exponential ($\beta = 1$), but it also highlights that the conclusion is connected with a high level of uncertainty.

Another interesting observation related to these measurements are the values of the observed lifetimes, which are significantly below the ideal PL decay curve, see Figure S4(a), suggesting a high influence of slow non-radiative relaxation in these samples with iQYs in the range of only a few percent $A_{\mathrm{PL}} = (0.01 \pm 0.1) A_{\mathrm{PL}}^{\mathrm{ideal}}$. This conclusion well agrees with a subsequent report on blinking analysis[11] by the same group.

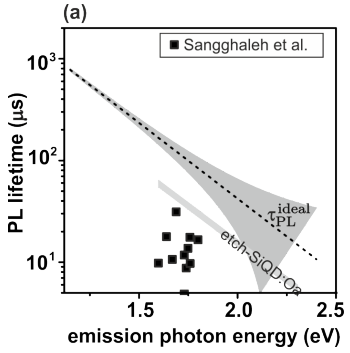

Figure S4: (a) Comparison of single-QD PL lifetimes[10] with the PL trends discussed in the main text (see Figure 2(b)).

References

(1) Miura, S.; Nakamura, T.; Fujii, M.; Inui, M.; Hayashi, S. Size dependence of photoluminescence quantum efficiency of Si nanocrystals. *Phys. Rev. B* **2006**, *73*, 245333.

(2) Greben, M.; Khoroshyy, P.; Liu, X.; Pi, X.; Valenta, J. Fully radiative relaxation of silicon nanocrystals in colloidal ensemble revealed by advanced treatment of decay kinetics. *J. Appl. Phys.* **2017**, *122*, 034304.

(3) Valenta, J.; Greben, M.; Dyakov, S. A.; Gippius, N. A.; Hiller, D.; Gutsch, S.; Zacharias, M. Nearly perfect near-infrared luminescence efficiency of Si nanocrystals: A comprehensive quantum yield study employing the Purcell effect. *Sci. Rep.* **2019**, *9*, 11214.

(4) Sangghaleh, F.; Sychugov, I.; Yang, Z.; Veinot, J. G. C.; Linnros, J. Near-Unity Internal Quantum Efficiency of Luminescent Silicon Nanocrystals with Ligand Passivation. *ACS Nano* **2015**, *9*, 7097–7104.

(5) Kalkman, J.; Gersen, H.; Kuipers, L.; Polman, A. Excitation of surface plasmons at a SiO_2Ag interface by silicon quantum dots: Experiment and theory. *Phys. Rev. B* **2006**, *73*, 075317.

(6) Liu, X.; Zhang, Y.; Yu, T.; Qiao, X.; Gresback, R.; Pi, X.; Yang, D. Optimum Quantum Yield of the Light Emission from 2 to 10 nm Hydrosilylated Silicon Quantum Dots. *Part. Part. Syst. Char.* **2016**, *33*, 44–52.

(7) Greben, M.; Valenta, J. Note: On the choice of the appropriate excitation-pulse-length for assessment of slow luminescence decays. *Rev. Sci. Instr.* **2016**, *87*, 126101.

(8) Greben, M.; Khoroshyy, P.; Sychugov, I.; Valenta, J. Non-exponential decay kinetics: correct assessment and description

illustrated by slow luminescence of Si nanostructures. *Appl. Spectr. Rev.* **2019**, *54*, 758–801.

(9) K. Kůsová,; Popelář, T. On the importance of onset times and multiple-wavelength analysis of photoluminescence decays. *J. Appl. Phys.* **2019**, *125*, 193103.

(10) Sangghaleh, F.; Bruhn, B.; Schmidt, T.; Linnros, J. Exciton lifetime measurements on single silicon quantum dots. *Nanotechnology* **2013**, *24*, 225204.

(11) Pevere, F.; Sangghaleh, F.; Bruhn, B.; Sychugov, I.; ; Linnros, J. Rapid trapping as the origin of nonradiative recombination in semiconductor nanocrystals. *ACS Photonics* **2018**, *5*, 2990–2996.